# RSC Advances

ROYAL SOCIETY
OF CHEMISTRY

www.rsc.org/advances

# Cooling-induced formation of honeycomb patterns on pre-cast PMMA films at low temperatures
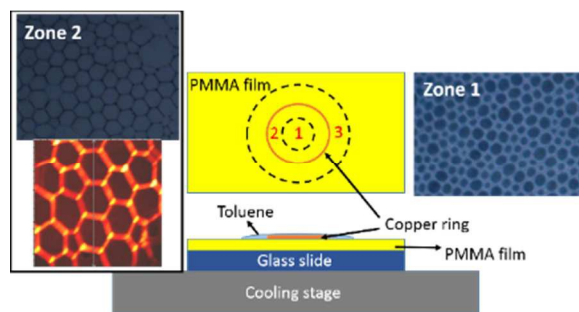
*Wei Sun and Fuqian Yang\**

Materials Program, Department of Chemical and Materials Engineering

University of Kentucky, Lexington, KY 40506, United States

fyang2@uky.edu

**Table of contents entry**

Surface patterns formed on pre-cast PMMA films. A typical AFM image shows the hexagon network.

**Abstract**

Using a copper ring to control the evaporation of toluene droplets on the surface of PMMA films at low temperatures, honeycomb patterns of various topologies are formed in different regions. The honeycomb of largest pore size is around the center area, and the pore size decreases gradually as the distance to the center increases. The effects of the film thickness and the substrate temperature on the honeycomb structures are examined. The pore size increases with the decrease of the film thickness. Hexagonal networks are formed at the substrate temperature of ~8 ºC. The "breath figure" mechanism is used to explain the formation of the honeycomb structures. The patterns formed on PS films under the same experimental conditions are examined, which are significantly different from the patterns formed on PMMA films.

**Keywords:** polymer film; honeycomb structures; evaporation; hexagonal network.

## Introduction

Evaporating-induced surface patterning is an effective and efficient method to construct well-ordered surface structures. By evaporating a droplet of a polymer solution or a particle suspension on a non-dissolvable substrate [1] or a pure solvent droplet on a dissolvable polymer film [2], self-assembled patterns are formed through the "stick-slip" motion of the contact line, which is associated with the "coffee ring" effect [3]. Various patterns, such as concentric rings [4], parallel straight stripes [5, 6], gradient arcs, spokes [7], etc. have been constructed, using different templates. One can alter the geometrical characteristics of the surface patterns by controlling the solution concentration, template, film thickness, solvent, molecular weight, etc.

In addition to the patterns mentioned above, honeycomb structures, which have potential in various applications [8], can also be fabricated via the solution evaporation [9, 10]. When a droplet of a polymer solution, in which the solvent is immiscible with water, is placed on a substrate and evaporates at relatively high humidity, the evaporation of the droplet can introduce a temperature difference between the droplet surface and ambient environment, leading to the condensation of small water droplets onto the surface of the solution droplet. The water droplets condensed can arrange into a hexagonal network which serves as a template for the formation of honeycomb patterns [11]. There are many factors, including ambient humidity [12], solvent [9], evaporation rate [13], solution concentration [12, 14], molecular weight [12, 15], surfactant [16], etc., which control the formation and geometric configurations of the "water-assisted" honeycomb patterns. Many materials, including hydrophobic polymer, amphiphilic copolymer [17], organic and saccharine-containing polymers [18], inorganic/organic hybrid [19], small organic molecules [20], etc., have been used to form honeycomb patterns via evaporation at relatively high temperatures. However, there is no report of the formation of honeycomb patterns at low temperatures.

Following the technique to form gradient concentric rings via the evaporation of a toluene droplet at room temperature [21], we develop a "ring-on-film" system, in which a pure toluene droplet is placed on the surface of a pre-cast PMMA film coated on a glass slide and a copper ring is used to confine the toluene droplet. Instead of using the air (moisture) flow for the condensation of water, a cooling stage is used to limit the evaporation of the toluene droplet at temperatures much lower than ambient temperature, which allows the condensation of water on the surface of the toluene droplet and leads to the formation of honeycomb-like patterns. The effects of the film thickness, the size of the copper ring and temperature are examined. In

addition, the surface patterns formed on PS films, using the same template structure, are reported. It is worth pointing out that the system consists of a pure solvent and a pre-cast dissolvable film in contrast to the use of polymer solutions on non-dissolvable substrate systems, as reported in literature.

**Experimental detail**

Preparation of polymer films

The PMMA films were prepared, using a spin-coating process at room temperature. The solution for spin-coating was PMMA (Mw=35000) (Fisher Scientific, Pittsburgh, PA) in toluene (Fisher Scientific, Pittsburgh, PA). The spin-coating was performed on a spin coater (WS-400B-6NPP/LITE, Laurell Technologies Corp., North Wales, PA) at 2000 rpm. PMMA thin films of different thicknesses were obtained, using different solution concentrations (~90 nm from 1 wt% solution, ~140 nm from 2 wt% solution, and ~290 nm from 5 wt% solution, as measured by atomic force microscopy). Also, PS films were spin-coated on pre-cleaned glass slides, using a 5 wt% PS (35000, Sigma-Aldrich) solution in toluene and the same spin-coating parameters as the spin-coating of the PMMA films.

Formation of hexagon network on pre-cast PMMA films

The surface patterns were constructed via the evaporation of a toluene droplet on a pre-cast PMMA film, using a copper ring to confine the droplet. The evaporation temperature was controlled by a cooling stage. Figure 1a shows the experimental setup. A toluene droplet (~6 µL) was placed on the surface of a pre-cast PMMA film coated on a glass slide, and a copper ring with a wire diameter of 79 µm (30 AWG) was used to confine the droplet. The glass slide was then moved onto a cooling stage immediately. Note that the cooling stage had already reached the pre-set temperature before the glass slide was placed on it. The evaporation of the toluene droplet took place in an ambient environment (temperature: 24.8 ºC; humidity: 35%). The surface temperature of the PMMA films was controlled in the range of -3.5 to 8 ºC, and the real-time temperature of the surface of the pre-cast PMMA films during the evaporation was monitored, using a thermocouple. The surface morphology of the surface patterns formed in different areas (as noted in Fig. 1a) after complete evaporation was examined by an optical microscope, and the height of the patterns was characterized by an atomic force microscope (AFM). Copper rings of different diameters (1.45, 2.90, and 3.75 mm) were used to study the size effect of the copper ring on the patterns. The optical images of the surface patterns were

analyzed, using Image-pro plus, to determine the average size and size distribution of the surface patterns. Fast Fourier Transform (FFT) was also carried out, using Image-pro plus.
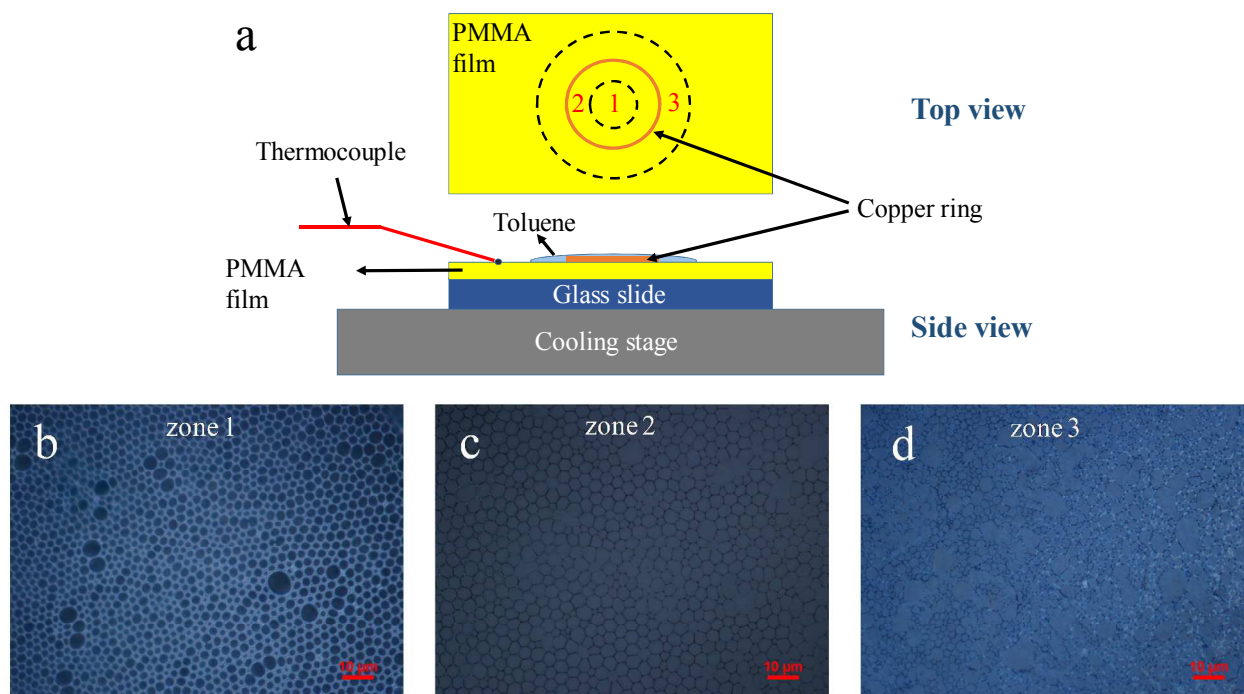
## Results and Discussions



**Figure 1.** (a) Schematic of experimental setup; (b-d) surface patterns formed in the zones of 1-3 as labeled in Fig. 1a, respectively (film thickness: ~140 nm, diameter of the copper ring: 1.45 mm, surface temperature of the film at equilibrium: ~8 ℃)

Figure 1b-d show the surface patterns formed on a pre-cast PMMA film of ~140 nm in thickness via the evaporation of a toluene droplet. The surface temperature of the PMMA film at equilibrium was 8 ℃. In the circular area of about 0.4 mm in radius around the center of the copper ring (noted as zone 1 in Fig. 1a), irregular holes with non-uniform distribution of hole sizes were formed. A few large holes are observed, but most of the holes are small. In zone 2, the surface pattern exhibits a hexagon network with some local defects, and there is a size distribution of the hexagons. In zone 3, i.e. the area outside the copper ring, the surface patterns become more irregular. Both irregular holes of relatively large sizes and local hexagon networks can be found in some small areas.
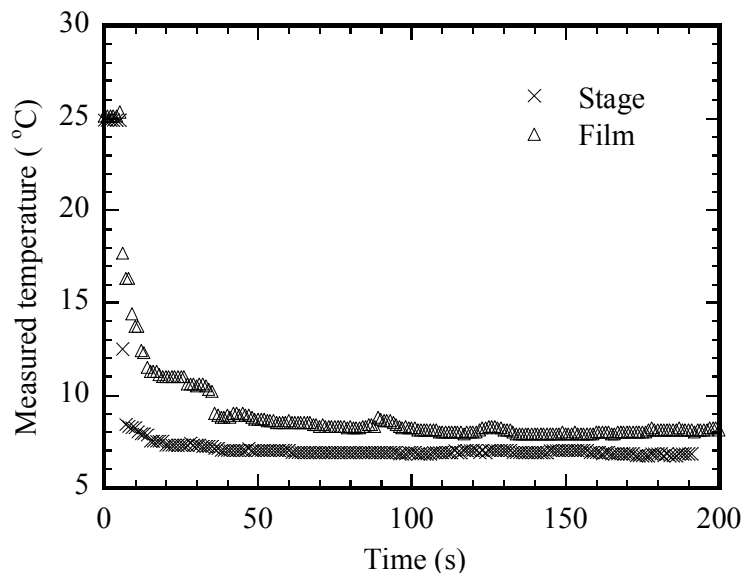
**Figure 2.** Temporal evolution of the temperature of the cooling stage and the surface temperature of a pre-cast PMMA film of ~140 nm thickness

Using a thermocouple, the temporal evolution of the temperatures of the cooling stage and the structure consisting of a pre-cast PMMA film and a glass slide was recorded, respectively. Figure 2 shows the variation of the measured temperatures of the cooling stage and the surface temperature of a pre-cast PMMA film of ~140 nm thickness with time for the cooling stage at a pre-set temperature of 5 ºC. Note that the cooling stage had already reached thermal equilibrium state at 5 ºC and the probe of the thermocouple was at 25 ºC before the measurement. It took about 30 s for the probe/cooling stage to reach local thermal equilibrium at ~6.8 ºC, while it took about 50 s for the probe/PMMA/glass structure to reach local thermal equilibrium at ~8 ºC. There exists a temperature difference between the cooling stage and the surface of the PMMA film, which was due to the difference between the pre-set temperature and the ambient temperature and the thermal resistances of the glass slide and the PMMA film to heat flow. This result suggests that toluene droplets were at a non-thermal equilibrium state during the evaporation in addition to the evaporation-induced temperature difference between the contact front and the evaporation surface.

Generally, a toluene droplet will spread and evaporate simultaneously after being placed on the surface of a PMMA film at ambient temperature. The copper ring will confine the spreading of the toluene droplet and keep the moving front circular if there are no local defects to pin the

motion of the contact line. Following the placement of the toluene droplet, the structure consisting of the droplet, PMMA film, and a glass substrate is moved to a cooling state with a temperature less than ambient temperature. This will cause the condensation of water on the surface of the toluene droplet and the surface of the PMMA film not covered by the toluene droplet. The condensation of water on the surface of the PMMA film will reduce the resistance to the motion of the contact line and accelerate the spreading of the toluene droplet. It also can introduce local disturbance, due to non-uniform condensation of water, to the motion of the contact line and cause the contact line to deviate from a circular-like contour to an irregular one. The water condensation can only limit the evaporation of the toluene confined by the copper ring through the formation of water micro-droplets. It is known that the density of water is larger than that of toluene and there is a deformable layer formed at the interface between the toluene and the PMMA film due to the penetration of toluene into the PMMA film [6]. The water droplets will cause deformation of the deformable layer, which leads to the formation of vertical channels, i.e. the PMMA ridges, after the evaporation of the toluene. Note that the vertical channels provide the space for the evaporation of the toluene. Since water is immiscible with toluene, the water droplets will continuously occupy the same positions until they are completely evaporated. This route eventually leads to the formation of holes on the surface of the PMMA film, as demonstrated in Figs. 1b-d.

The use of a copper ring to confine the spreading and evaporation of the toluene droplet has made the evaporation process different from the evaporation of a droplet without any confinement, which can be in a mode of constant contact area, constant contact angle, or a mixed mode with only one contact line. With the confinement of the copper ring, the contact line outside the copper ring moves towards the copper ring after spreading, and the surface of the toluene droplet inside the copper ring evolves gradually from convex to concave during evaporation. This allows the accumulation of water droplets on the surface of the toluene droplet and the motion of water droplets towards the center of the copper ring (i.e. the vertex of the surface of the toluene droplet). The motion of water droplets introduces the collision and merge of water droplets to form larger water droplets in contrast to the formation of uniform water droplets on a smooth, flat surface. The large droplets formed through random merge of small droplets lead to the wide distribution of the porous structures in zone 1. Note that the motion of water droplets on the surface of the toluene droplet and the evaporation of toluene also induce

micro-flow inside the toluene droplet, and the micro-flow plays a role in controlling the motion of water droplets. In contrast, the water droplets in zone 2 are at a relatively stationary state due to the nonslip condition imposed by the copper ring, which limits the collision and merge of water droplets and water droplets have relatively uniform size. The water droplets of relatively uniform size form a water-droplet-template, leading to the formation of well-ordered hexagonal network in zone 2.
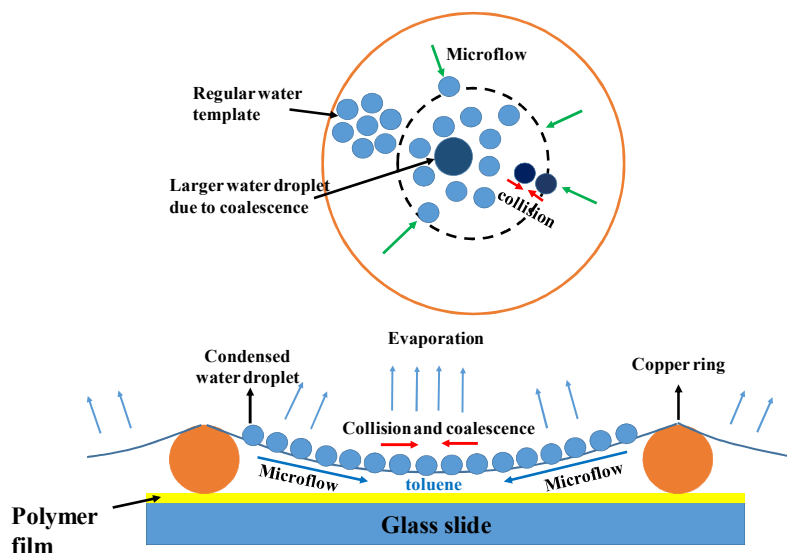


**Figure 3.** Schematic illustration of the formation of a breath figure template during the evaporation of a toluene droplet on a PMMA film placed on a cooling stage

The hexagon patterns formed on the PMMA films can be explained by the "breath figure" mechanism [22]. Figure 3 shows a schematic illustration of the formation of a water droplet template. As shown in Fig. 2, the surface temperature of the PMMA film was less than ambient temperature after placing the droplet/film/glass system on the surface of a cooling stage. It is expected that the surface temperature of the toluene droplet is also less than ambient temperature. Due to the temperature difference between ambient temperature and the temperature of the toluene droplet, water condensation on the surface of the toluene droplet occurs even for a relative humidity of 35% and the nucleation of water droplets takes place when the droplet sizes are larger than the critical size. The droplets gradually grow with time and arrange into hexagonal configuration locally under the action of capillary force and the interaction between droplets [12]. With continuous evaporation of toluene, these water droplets gradually penetrate into

the compliant PMMA film, resulting in the formation of a porous PMMA film with a hexagonal pattern after both water and toluene evaporate completely.

The evolution of water droplets and the interaction between water droplets and the compliant substrate are a function of the experimental conditions, including film thickness, temperature, and film material. Their effects on the geometric characteristics of the surface patterns are examined and discussed below with the focus on the regular patterns formed inside the copper ring.
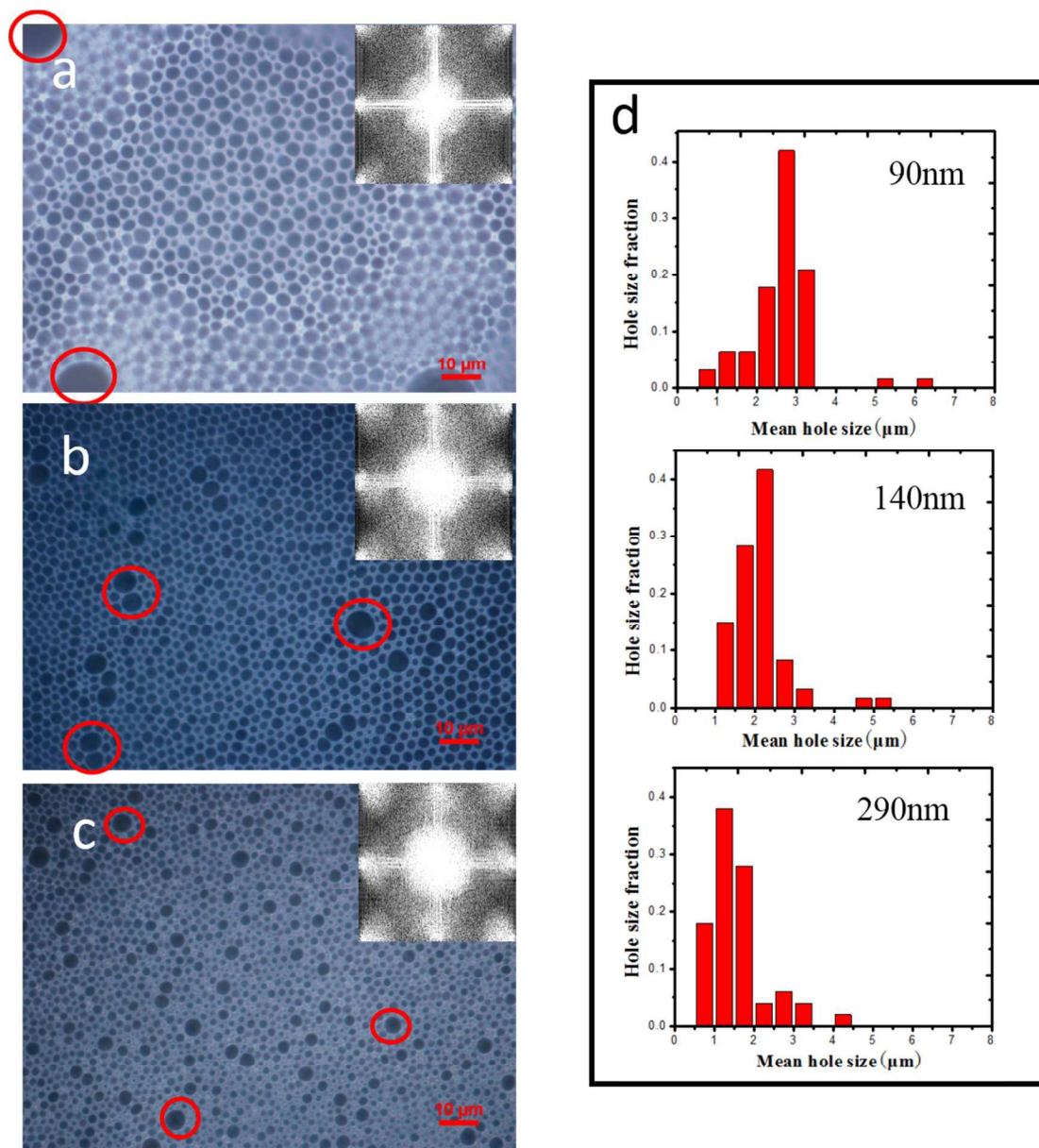


**Figure 4.** Surface patterns formed in zone 1 on different PMMA films; (a) ~90 nm in thickness, (b) ~140 nm in thickness and (c) ~290 nm in thickness; (d) size distribution of the holes formed

on the PMMA films (surface temperature of the PMMA at equilibrium: ~8 ºC, diameter of the copper ring: 1.45 mm). Inserted images are the Fast Fourier Transform (FFT) patterns of the corresponding surface patterns.
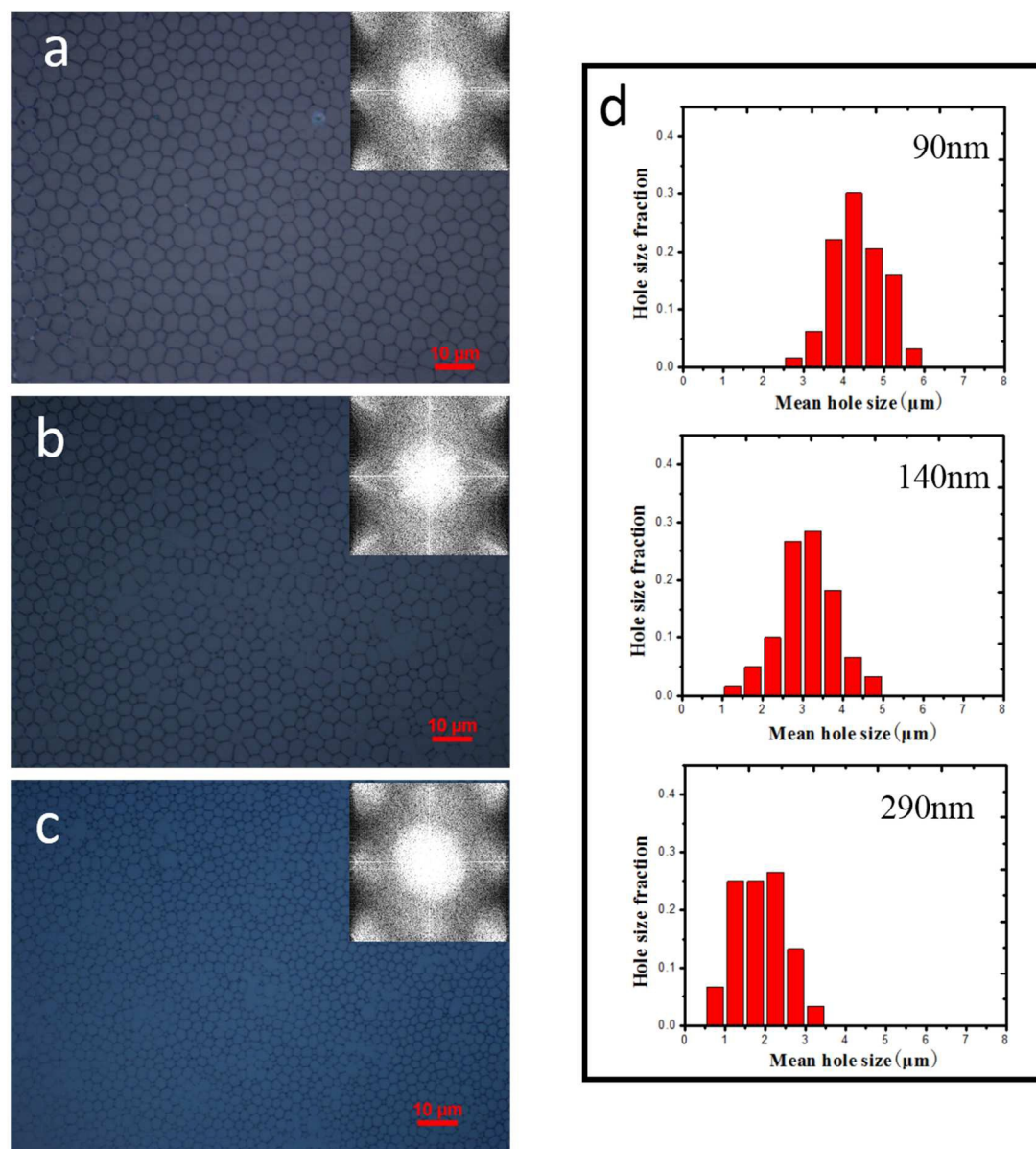


**Figure 5.** Patterns formed in zone 2 on different PMMA films; (a) ~90 nm in thickness, (b) ~140 nm in thickness and (c) ~290 nm in thickness; (d) size distribution of the holes formed on the PMMA films (surface temperature of the films at equilibrium: ~8 ºC, diameter of the copper ring: 1.45 mm). Inserted images are the FFT patterns of the corresponding surface patterns.

Effect of film thickness

Figures 4a-c show the patterns formed in zone 1 for PMMA films of three thicknesses. The surface temperature of the films at equilibrium was ~8 ºC. Holes of multiple sizes were formed on the PMMA films of ~90, ~140 and ~290 nm in thickness are non-uniform. Several holes, as circled by red circles, are relatively large, and most holes are relatively small. Figure 4d shows the size distributions of the holes formed on the PMMA films of three thicknesses. Broad distribution of the hole sizes is observed for all the three films. Generally, the holes in the thicker films have smaller sizes than the holes in the thinner films. Most holes have the sizes in the range of 2-3.5 µm for ~90 nm films, 1-2.5 µm for ~140 nm films, and 0.5-2 µm for ~290 nm films, respectively. There are only small portion of holes with larger sizes for all the films.

The surface patterns in zone 2 on all the films appear more likely as a hexagon network, as shown in Figs. 5a-c, for water condensed on the films at an equilibrium surface temperature of ~8 ºC. The surface pattern formed on the thinnest films (~90 nm) has a nearly perfect hexagon network, while some local defects can be observed on thicker films. The average size of a single unit (hexagon) decreases with the increase of the film thickness, which is ~4.37±0.55 µm for ~90 nm films, ~2.96±0.91µm for ~140 nm films, and ~1.83±0.57 µm for ~290 nm films. Comparing with the surface patterns formed in zone 1 for the same film thickness, one can note that the sizes of the hexagon holes in zone 2 are more uniform. Figure 5d shows the size distribution of the hexagons in zone 2. About 86% hexagonal holes have size in the range of 2.5-5.5 µm for ~90 nm films, about 84% hexagonal holes have sizes in the range of 2-4 µm for ~140 nm films, and about ~90% hexagonal holes have sizes in the range of 1-3 µm for ~290 nm films. There is no significant change in the sizes of the hexagon holes formed in zone 2.

Fast Fourier Transform (FFT) was used to analyze the ordering of the holes. The FFT diffraction patterns, as shown in the inset in Figs. 4a-c and Figs. 5a-c, reveal a square arrangement of both the nearly circular holes in zone 1 and the hexagonal holes in zone 2. It is known that hexagonal packing is a usual packing mode of holes, which is free-energy favored [23]. The mechanism for the square arrangement is unclear, which might be attributed to the low substrate temperature. The low surface temperature of the toluene droplet can lead to a fast condensation of water droplets and reduce the mobility of the water droplets, resulting in a packing mode of less compact. Other factors, i.e. micro-flow inside the toluene droplet and the

evaporation rate of the toluene might also play important roles in the packing of the water droplets and influence the arrangement of the holes and the surface patterns.
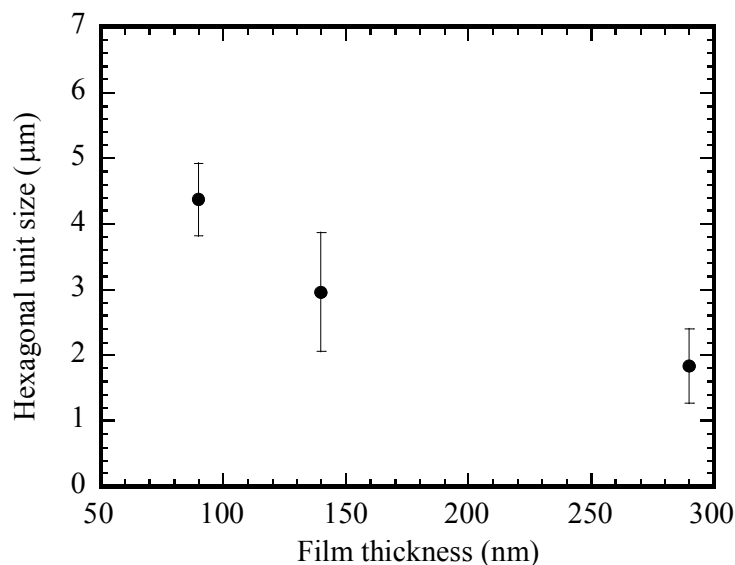


**Figure. 6** Size variation of the hexagonal units with the PMMA film thickness (copper ring size: 1.45 mm, surface temperature of the film at equilibrium state: ~8.0 ºC).

Figure 6 shows the variation of the average size of the hexagonal units with the thickness of the PMMA film. The average size of the hexagonal units decreases with the increase of the film thickness when other experimental conditions remain the same. Generally, the size of a water droplet is determined by the nucleation size and the growth rate. From the theory of thermodynamics, the critical radius for the formation of a water droplet is [24]

$$R_{cr} = \frac{2\Omega\gamma}{kT_s \ln(p_s / p_\infty)} \tag{1}$$

where $R_{cr}$ is the critical radius of water droplets, $\gamma$ is the surface tension, $\Omega$ is the volume per one water molecule, $k$ is the Boltzmann constant, $T_s$ is the surface temperature of the toluene droplet, $p_s$ is the vapor pressure on the surface of the toluene droplet, $p_\infty$ is the vapor pressure of environment. The growth rate of a water droplet is dependent on the absorption and diffusion of water molecules, which can be expressed as

$$\frac{dR}{dt} = A(T_\infty - T_s)^n \tag{2}$$

where $R$ is the radius of the water droplet, $t$ is time, $T_\infty$ is the temperature of the environment, $n(>0)$ is a power index, and $A$ is a coefficient. Note that Beysens et al. [25] suggested $n=1$, and Xu

et al. [12] suggested *n*=0.8. Generally, the PMMA concentration near the toluene surface is higher for a thicker film due to the fast diffusion of toluene into the PMMA film than for a thinner film. The solvent (toluene) in a more concentrated solution has lower vapor pressure, resulting in slower evaporation and a higher temperature on the surface of the toluene surface over a thicker PMMA film than that of a thinner PMMA film. Note that the surface temperatures of PMMA films at local equilibrium state were $8.0\pm0.1$, $8.0\pm0.2$ and $8.2\pm0.2$ for the PMMA films with thicknesses of ~90, ~140, and ~290 nm, respectively, which indirectly supports that the surface of a toluene droplet of the same size over a thicker PMMA film might have a slightly higher temperature than that on a thinner PMMA film. According to Eqs. (1) and (2), both the critical radius for the formation of water droplets and the growth rate of water droplets on the surface of a toluene droplet over a thicker PMMA film thus are smaller than those on a thinner PMMA film. As we observed, there is no significant difference in the total evaporation time of toluene droplets of the same size on PMMA films of different thicknesses. One can conclude from Eqs. (1) and (2), smaller water droplets will be formed on a thicker PMMA film, which leads to the formation of a hexagonal network with hexagonal units of smaller size in accord with the experimental observation.
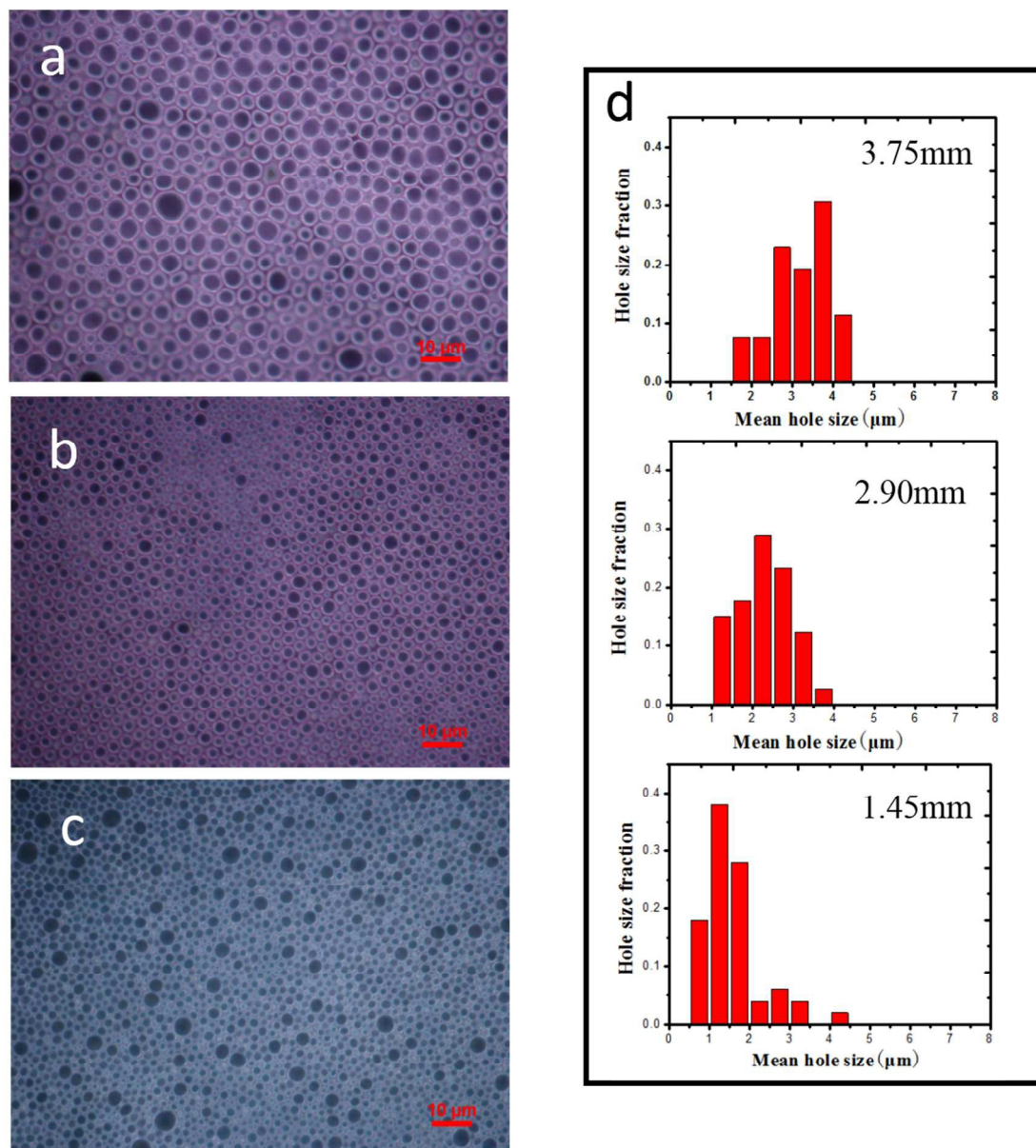
**Figure 7.** Surface patterns formed in zone 1 on PMMA films with copper rings of different sizes (a) ~3.75 mm in diameter, (b) ~2.90 mm in diameter, and (c) ~1.45 mm in diameter; (d) size distribution of the holes formed on the PMMA films (film thickness: 290 nm, surface temperature of the PMMA at equilibrium: ~8 ℃)
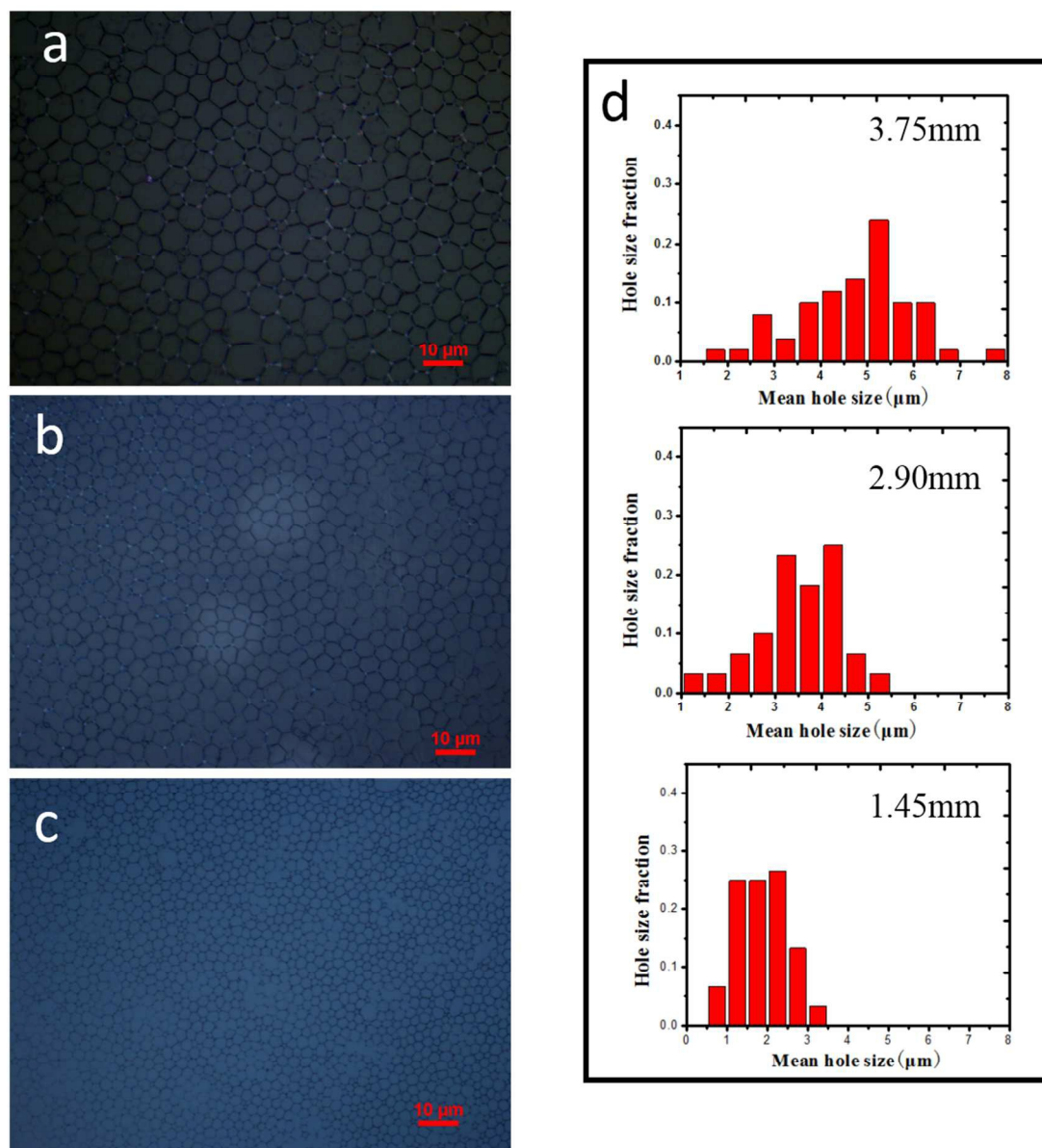
**Figure 8.** Surface patterns formed in zone 2 on PMMA films with copper rings of different sizes (a) ~3.75 mm in diameter, (b) ~2.90 mm in diameter, and (c) ~1.45 mm in diameter; (d) size distribution of the holes formed on the PMMA films (film thickness: 290 nm, surface temperature of the films at equilibrium: ~8 ºC)

Effect of copper ring size

Figures 7a-c show the surface patterns formed on PMMA films of ~290 nm in thickness with copper rings of different sizes. The surface temperature of the film is 8 ºC. Holes of multiple

sizes are observed for all the three copper ring sizes. As shown in Fig. 7d, the holes formed with all the three copper rings have broad size distributions, while the hole size is relatively more uniform for the patterns formed with a smaller copper ring than those formed with a larger copper ring. The hole size also has a decreasing tendency with the decrease of the size of the copper ring. The hole size is in the range of 2.5-4.5 μm for the ~3.75 mm copper ring, 1-3.5 μm for the 2.90 mm copper ring, and 0.5-2 μm for the 1.45 mm copper ring, respectively.

The hexagonal network is formed in zone 2 for the templates with the three copper rings, as shown in Figs. 8a-c. Generally, the size of the hexagons decreases with the decrease of the size of the copper ring. The average size of hexagonal units is ~4.72±1.20 μm for the ~3.75 mm copper ring, ~3.56±0.71 μm for the 2.90 mm copper ring, and ~1.83±0.57 μm for the 1.45 mm copper ring, respectively. Figure 8d shows the size distribution of the hexagon units in zone 2. The patterns formed with a smaller copper ring have narrower size distribution than those formed with a larger copper ring. About 92% hexagonal units have sizes in the range of 2.5-6.5 μm for the ~3.75 mm copper ring, 90% of the hexagonal units have sizes in the range of 2-5 μm for the ~2.9 mm copper ring, and 90% hexagonal units have sizes in the range of 1-3 μm for the ~1.45 mm copper ring, respectively.
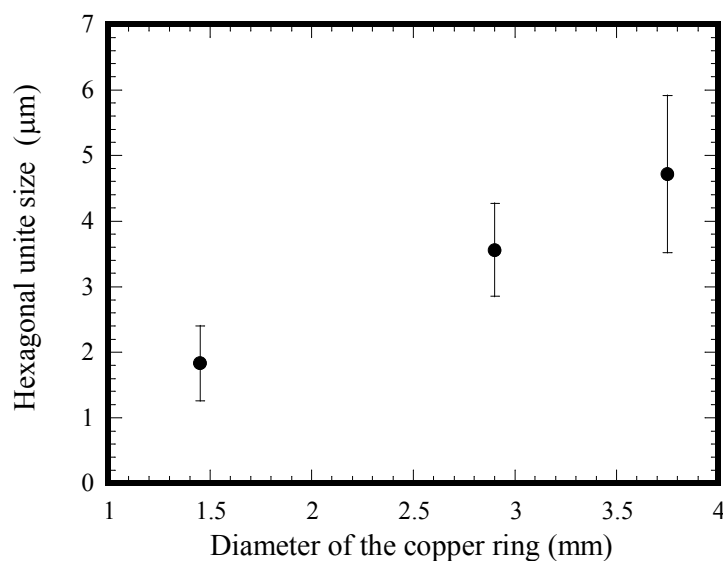


**Figure 9.** Size variation of the hexagonal units with the copper ring diameter (film thickness: 290 nm, surface temperature of the film at equilibrium state: ~8.0 ℃).

As shown in Fig. 9, the average size of the hexagonal units increases with the increase of the copper ring size. The mechanism for this phenomenon is very complicated, and it might be closely related to the geometry of the toluene droplet limited by the template (copper ring). Without any templates, the toluene droplet can wet a PMMA film well and form a very thin liquid film. With the presence of a copper ring, the liquid film will curve up in the area near the copper ring due to the confinement effect [26]. A decreasing gradient of the thickness of the toluene liquid film from the copper wire to the center of the copper ring is introduced, leading to a concave surface of the toluene film inside the copper ring, as shown in schematic illustration in Fig. 3. The thickness of the toluene film inside a larger copper ring is expected to be smaller than that within a smaller copper ring of the same wire size, especially for the region near the center, due to a larger distance to the copper ring. As the toluene liquid film is placed between the warmer air and the cooler substrate, there is a temperature gradient within the toluene in the direction parallel to the surface normal. For a thinner toluene film, the temperature of the top surface $T_s$ is lower than that of a thicker toluene film since the surface is closer to the cold substrate. Thus, the toluene film confined by a larger copper ring has a cooler surface. According to Eq. (1), the critical radius for the formation of a water droplet is larger for the case with a larger copper ring, which partially contributes to the larger sizes of the units formed with a larger copper ring. In addition, the size of the copper ring also affects the growth behavior of water droplets, the evaporation of the toluene droplet, the micro-flow inside the toluene droplet etc., which determine the geometrical characteristics of the surface patterns. Due to the limit of experimental conditions, we will address the effects of some other factors in the future work.
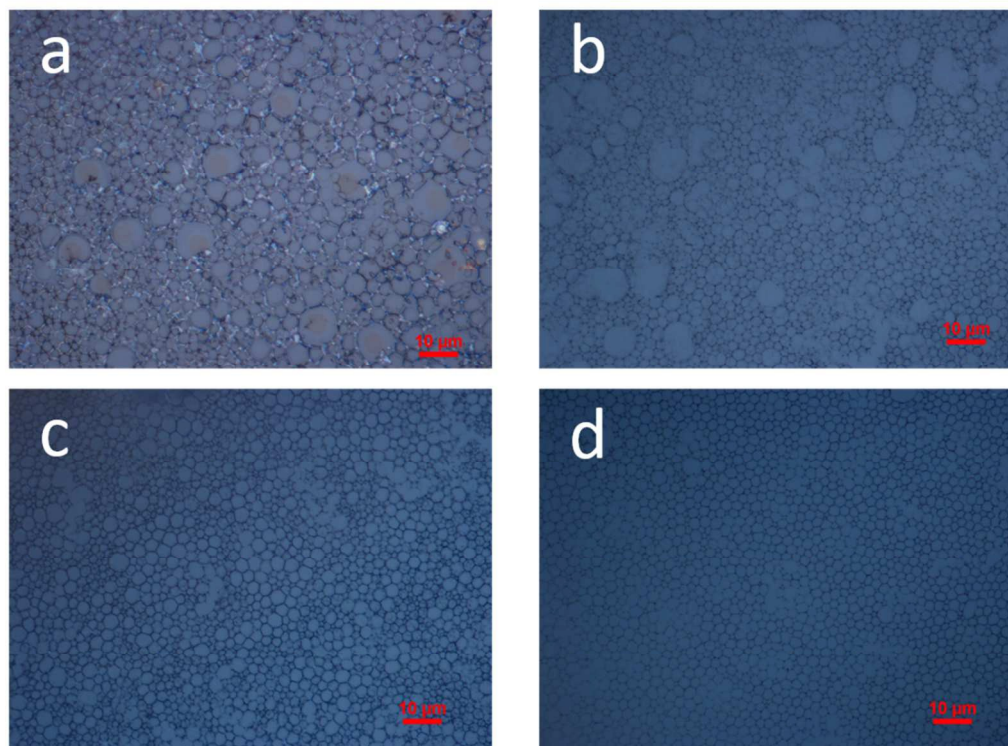
**Figure 10.** Surface patterns formed in zone 2 on the PMMA films of ~290 nm film thickness at four equilibrium temperatures; (a) ~3.5 ºC, (b) ~1.8 ºC, (c) ~6.0 ºC and (d) ~8.0 ºC (size of the copper ring: 1.45 mm).

Effect of substrate temperature

Figure 10 shows the surface patterns formed in zone 2 on the PMMA films of ~290 nm film thickness at four equilibrium temperatures. The size of the copper ring is 1.45 mm. At the temperature of -3.5 ºC, the surface patterns were random and disorder, while at the temperature of ~8 ºC, the surface patterns became well-ordered. Increasing the temperature introduced a transition of the surface patterns from disordered structures to well-ordered hexagon networks. Note that well-ordered concentric rings instead of hexagon networks will be formed at room temperature [21]. The morphology of the holes changes from irregular shape to uniform and regular hexagon.

Such behavior likely is associated with the temperature dependence of the water condensation. A lower temperature will lead to a higher condensation (nucleation) rate and a higher growth rate of water droplets than a higher temperature. This trend will cause the random migration of water droplets on the surface of a toluene droplet and increase the frequency of

collision between water droplets, which will result in the formation of water droplets of different sizes. The sinking of water droplets of different sizes into the deformable PMMA film leads to the formation of the honeycomb structure with a wider distribution of hole sizes at lower temperatures than at higher temperatures. A water-droplet-template of uniform size results in the formation of a hexagonal network on a PMMA film.
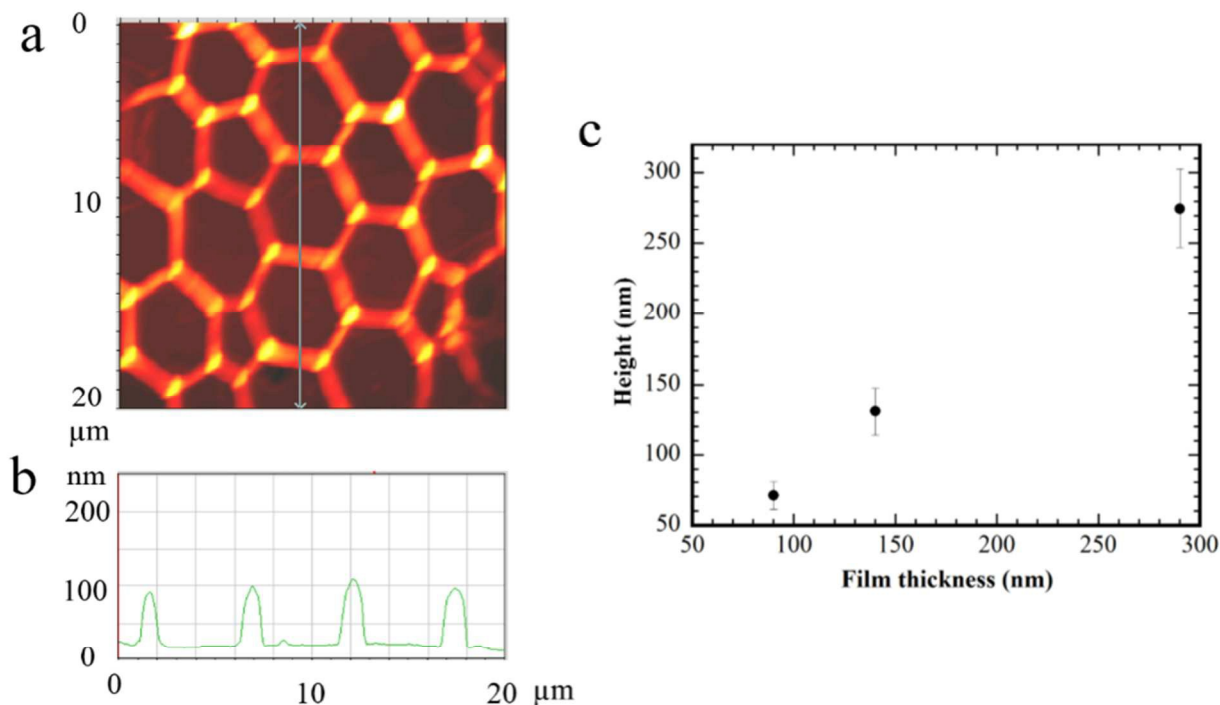


**Figure 11.** (a) A typical AFM image of the hexagon network formed in zone 2 on a PMMA film of ~90 nm thickness, (b) a line scan of the surface profile corresponding to the line in (a), and (c) variation of the wall height of the hexagon network with the film thickness (surface temperature of the film at equilibrium state: ~8.0 ºC)

Figure 11 shows a typical AFM image of the hexagon network formed in zone 2 on a ~90 nm PMMA film. The surface temperature of the film at equilibrium state was ~8.0 ºC. The surface pattern appears as a hexagon network in accord with the optical image shown in Fig. 10d. By drawing a line across the AFM image, one can determine the heights of the polymer ridges, i.e. the heights of the walls of the hexagons. Figure 8b shows the topology of the polymer ridges, corresponding to the line scan in Fig. 11a. It is clear that there is no significant difference in the

heights of the polymer ridges. Multiple scans were performed over the PMMA films of three different thicknesses. The measurement results are depicted in Fig. 11c. The height of the polymer ridges increases with increasing the thickness of the PMMA films.
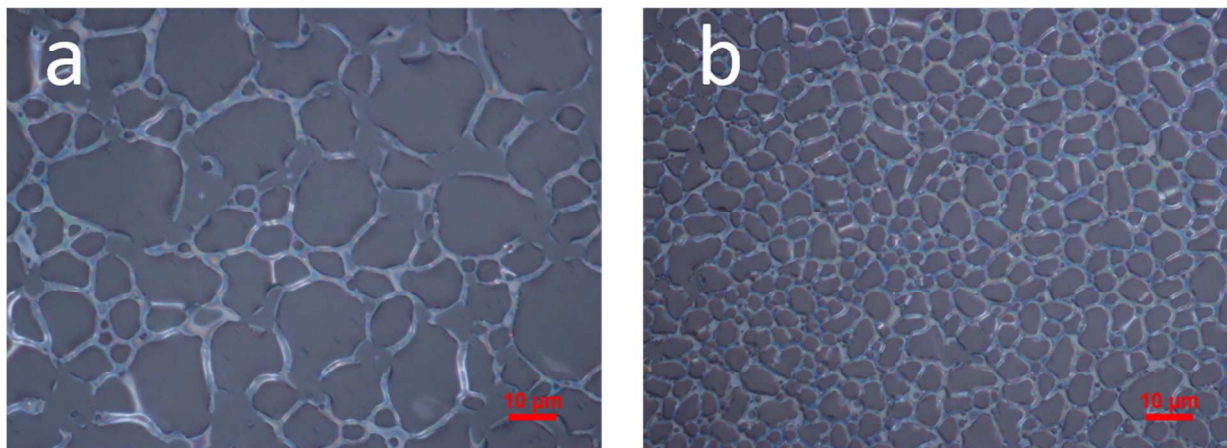


**Figure 12.** Surface patterns formed on a PS film via the evaporation of a toluene droplet: (a) in zone 1, and (b) in zone 2 (film thickness: ~290 nm, equilibrium temperature of the film surface: ~8.0 ℃, diameter of the copper ring: 1.45 mm)

The formation of surface patterns on a PS film was also examined, using the same experimental procedure. The thickness of the PS film was ~290 nm, and the diameter of the copper ring was 1.45 mm. The equilibrium surface temperature was ~8. 0 ℃. Figure 12 shows the typical surface patterns formed. Comparing Fig. 12 with Figs. 7 and 8, one can note that the surface patterns formed on the PS film is significantly different from those on the PMMA films. The patterns in both zone 1 and zone 2 are irregular and the thickness of the polymer ridges is non-uniform. The average hole size in zone 2 is much smaller than that in zone 1.

Generally, the evaporation kinetics of toluene is dependent on the interaction between toluene and substrate. It is known that a thin PMMA film has a more favorable interaction with a native oxide surface on a Si wafer than thin a PS film. Similarly, it is expected that a PS film has a less favorable interaction with a glass surface than a PMMA film. Also, the polymer/solvent interaction parameter at room temperature are 1.13 for PS/toluene slightly less than 1.21 for PMMA/toluene [4]. Toluene is a better solvent for PS than for PMMA. When a toluene droplet is placed on the surface of a polymer film, i.e. either a PMMA film or a PS film, more toluene will penetrate into the PS film than the PMMA film and weaken the interaction between the PS film

and the glass substrate. This allows the water droplets condensed to squeeze more PS/toluene away than PMMA/toluene during the sinking of the water droplets into the polymer/toluene film. Due to a less favorable interaction between PS and a glass surface than that between PMMA and a glass surface, larger holes are formed on a PS film than on those on a PMMA film for the same experimental conditions.

**Conclusion**

In summary, we constructed honeycomb structures on pre-cast PMMA films via the evaporation of a toluene droplet on a PMMA film at low temperatures. Using a copper ring, we confined the spreading and evaporation of the toluene droplet on the surface of the PMMA film. Honeycomb structures with various topologies, including hexagonal network, were formed in different regions due to the formation of water-droplet-templates during the evaporation, which were dependent on the evaporation kinetics, micro-flow, and the interaction between water droplets. Near the center of the copper ring, holes with a broad size distribution were formed due to the coalescence of the water droplets. In the area away from the center inside the copper ring, regular hexagon networks were formed at the temperature of ~8 ºC. The average size of the hexagonal units increases with the decrease of the film thickness and with the decrease of the copper ring size, and the height of the polymer ridges increases with the increase of the film thickness. More regular patterns were obtained when the temperature of the cooling stage was relatively higher. Significantly different honeycomb structures were formed on a PS film from the PMMA films, which is likely due to that the interactions between PMMA and toluene and between PMMA and the glass substrate are different from those between PS and toluene and between PS and the glass substrate.

## References

1. J. Xu, J. F. Xia, S. W. Hong, Z. Q. Lin, F. Qiu and Y. L. Yang, *Physical Review Letters*, 2006, **96**.

2. W. Sun and F. Q. Yang, *Soft Matter*, 2014, **10**, 4451-4457.

3. R. D. Deegan, *Physical Review E*, 2000, **61**, 475-485.

4. M. Byun, S. W. Hong, F. Qiu, Q. Zou and Z. Lin, *Macromolecules*, 2008, **41**, 9312-9317.

5. H. Yabu and M. Shimomura, *Advanced Functional Materials*, 2005, **15**, 575-581.

6. W. Sun and F. Yang, *Langmuir*, 2014, **30**, 6548-6555.

7. B. Li, W. Han, M. Byun, L. Zhu, Q. Zou and Z. Lin, *ACS nano*, 2013, **7**, 4326-4333.

8. Y. Tian, S. Liu, H.Y. Ding, L.H. Wang, B.Q. Liu and Y.Q. Shi, *Polymer,* 2007, **48** 2338-2344.

9. O. Karthaus, N. Maruyama, X. Cieren, M. Shimomura, H. Hasegawa and T. Hashimoto, *Langmuir*, 2000, **16**, 6071-6076.

10. M. Hernández-Guerrero and M. H. Stenzel, *Polymer Chemistry*, 2012, **3**, 563-577.

11. M. Srinivasarao, D. Collings, A. Philips and S. Patel, *Science*, 2001, **292**, 79-83.

12. Y. Xu, B. Zhu and Y. Xu, *Polymer*, 2005, **46**, 713-717.

13. J. Peng, Y. Han, Y. Yang and B. Li, *Polymer*, 2004, **45**, 447-452.

14. H. Cong, J. Wang, B. Yu and J. Tang, *Soft Matter*, 2012, **8**, 8835-8839.

15. J. Li, Q.-L. Zhao, J.-Z. Chen, L. Li, J. Huang, Z. Ma and Y.-W. Zhong, *Polymer Chemistry*, 2010, **1**, 164-167.

16. X. Jiang, T. Zhang, L. Xu, C. Wang, X. Zhou and N. Gu, *Langmuir*, 2011, **27**, 5410-5419.

17. T. Nishikawa, J. Nishida, R. Ookura, S.-I. Nishimura, S. Wada, T. Karino and M. Shimomura, *Mater Sci Eng: C*, 1999, **8–9**, 495-500.

18. N. Maruyama, T. Koito, J. Nishida, T. Sawadaishi, X. Cieren, K. Ijiro, O. Karthaus and M. Shimomura, *Thin Solid Films*, 1998, **327–329**, 854-856.

19. O. Karthaus, X. Cieren, N. Maruyama and M. Shimomura, *Mater Sci Eng: C*, 1999, **10**, 103-106.

20. Y. Yu and Y. Ma, *Soft Matter*, 2011, **7**, 884-886.

21. W. Sun and F. Q. Yang, *J Phys Chem C*, 2014, **118**, 10177-10182.

22. L. Rayleigh, *Nature*, 1911, **86**, 416-417.

23. E. L. Thomas, D. J. Kinning, D. B. Alward and C. S. Henkee, *Macromolecules*, 1987, **20**, 2934-2939.

24. G. Kaptay, *Journal of Nanoscience and Nanotechnology*, 2012, **12**, 2625-2633.

25. D. Beysens, A. Steyer, P. Guenoun, D. Fritter and C. Knobler, *Phase Transitions: A Multinational Journal*, 1991, **31**, 219-246.

26. W. Sun and F. Yang, *Langmuir*, 2015, **31**, 4024-4031.